Supplementary Information

Superior low-temperature tolerant, self-adhesive and antibacterial hydrogels for wearable sensors and communicators

Enke Feng,‡* Xiaoqin Li,‡ Mengzhen Zhang, Xinxian Ma, Linan Cao and Zhiqiang Wu*

College of Chemistry and Chemical Engineering, Ningxia Normal University, GuYuan 756000, China.

‡These authors contributed equally to this work. They should thus be considered co-first authors.

*Corresponding authors: NXSFEKF@126.com (E, Feng); Wuzqnd@163.com (Z, Wu).

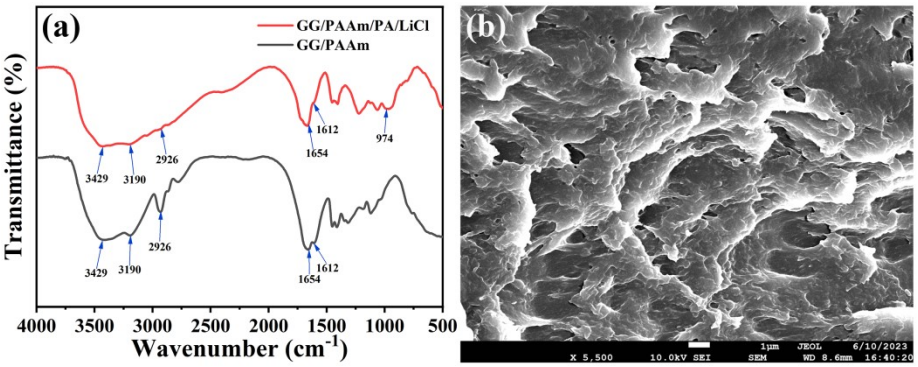

Fig. S1. (a) FT-IR spectra of the GG/PAAm and GG/PAAm/PA/LiCl hydrogels. (b) SEM image of the GG/PAAm/PA/LiCl hydrogel.

Fourier transforms infrared (FT-IR) spectroscopy of the GG/PAAm and GG/PAAm/PA/LiCl hydrogels was performed with a Thermo Scientific Nicolet iS5 spectrometer. In the spectrum of the GG/AAm hydrogel, the peaks at 3429 and 2926 cm^{-1} are attributed to the O-H stretching vibration and C-H asymmetric stretching vibration of GG (Fig. S1a).[1] Meanwhile, the characteristic peaks at 3190, 1654 and 1612 cm^{-1} are respectively assigned to the N-H stretching

vibration, C=O stretching vibration and N-H bending vibration of PAAm.[2-4] After the introduction of PA, the C-P-O stretching vibration of PA is found at the position of about 974 cm^{-1}.[5-6] Moreover, the introduction of PA also weakened the peaks at 3190, 2926 and 1612 cm^{-1}. Furthermore, the morphology of the GG/PAAm/PA/LiCl hydrogel was investigated by scanning electron microscopy (SEM, JSM-7610, Japan). As shown in Fig. S1b, it can be clearly seen that the hydrogel exhibits microscale pores and corrugated microstructures on the rough surfaces.

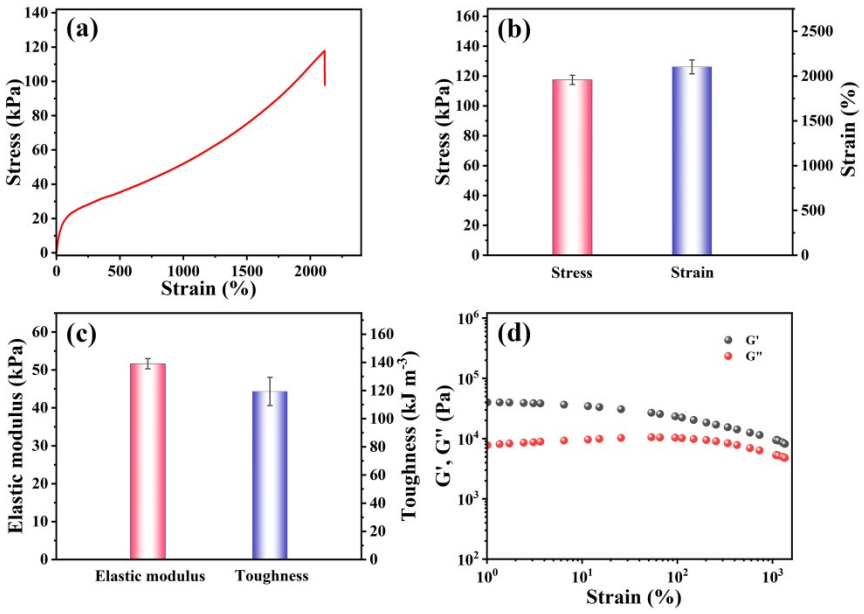

Fig. S2. (a) Stress-strain curves of the GG/PAAm/PA/LiCl hydrogel. (b) Fracture stress and strain of the GG/PAAm/PA/LiCl hydrogel. (c) Toughness and elastic modulus of the GG/PAAm/PA/LiCl hydrogel. (d) Storage modulus (G') and loss modulus (G") of the GG/PAAm/PA/LiCl hydrogel on strain amplitude sweep.

The elastic modulus was obtained by calculating a linear fit to the initial portion of the stress-strain curve (0% to 20%). The toughness was assessed by the extension work at fracture, which was obtained by integrating the area of the stress-strain curve. The rheological analysis was

performed by a rheometer (Haake Mars60). The sample was made into a circular sheet with a diameter of 20 mm and a thickness of about 2 mm, and the strain amplitude sweep measurement was conducted with the strain increasing from 1% to 1300% at a frequency of 1 Hz.

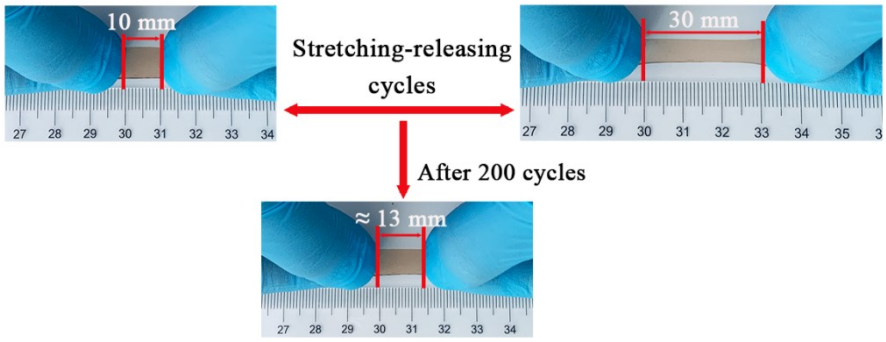

Fig. S3. The fatigue resistance of GG/PAAm/PA/LiCl hydrogel during 200 stretching-releasing cycles.

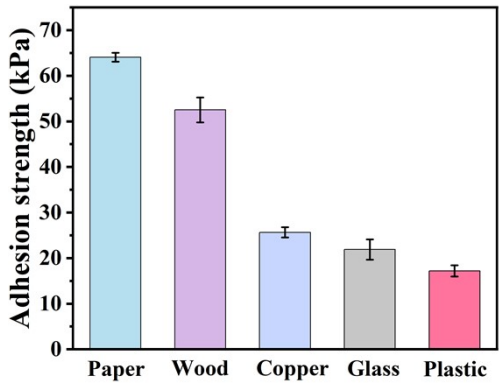

Fig. S4. Adhesion strength of GG/PAAm/PA/LiCl hydrogels on various substrates.

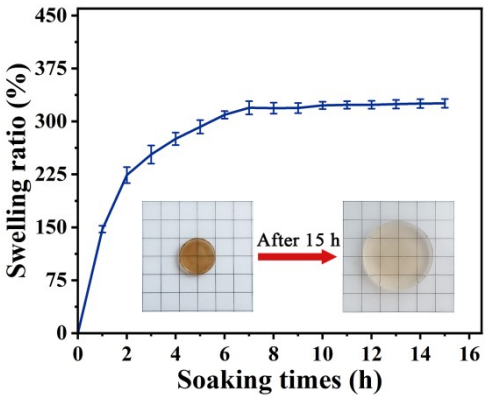

Fig. S5. The swelling property of the GG/PAAmPA/LiCl hydrogel in phosphate-buffered saline (PBS, pH = 7.4). The sample (diameter: 20 mm, thickness: 2 mm) was immersed in a phosphate-buffered saline (PBS, pH= 7.4) solution at room temperature and then the immersing sample was taken out for weigh after wiping with filter paper at a fixed interval.

References

1. Y. Wang, M. Yang and Z. Zhao, *Carbohydr. Polym.*, 2023, **310**, 120723.

2. H. Zhang, X. Wu, Z. Qin, X. Sun, H. Zhang, Q. Yu, M. Yao, S. He, X. Dong, F. Yao and J. Li, *Cellulose,* 2020, **27**, 9975-9989.

3. N. Li, J. Li, W. Sun, Y. Qiu and W. Chen, *ACS Appl. Polym. Mater.*, 2022, **4**, 5717-5727.

4. S. Ko, A. Chhetry, D. Kim, H. Yoon and J. Y. Park, *ACS Appl. Mater. Interfaces*, 2022, **14**, 31363-31372.

5. C. Liu, R. Zhang, P. Li, J. Qu, P. Chao, Z. Mo, T. Yang, N. Qing and L. Tang, *ACS Appl. Mater. Interfaces*, 2022, **14**, 26088-26098.

6. Z. Wang, Z. Ma, S. Wang, M. Pi, X. Wang, M. Li, H. Lu, W. Cui and R. Ran, *Carbohydr. Polym.*, 2022, **298**, 120128.